

Aging in granular columns

Author: Jordi Ferré Ortega

Facultat de Física, Universitat de Barcelona, Diagonal 645, 08028 Barcelona, Spain.

Advisor: Ramon Planet

Abstract: This work presents a study of the temporal evolution of granular matter confined in narrow columns. Grains are added into the containers and let them evolve for 6 to 10 hours. Two temporal regions are identified: an initial relaxation independent of volume with an average relaxation time of $\tau \approx 900$ s; and long-term regime where the system saturates and shows fluctuations around this saturation mass. These fluctuations are characterised by distributions with a fourth moment which slightly differs from the one of a Gaussian distribution. Both responses have been analysed for different added masses that correspond to different mechanical properties of the granular pile. Finally, it is observed that different experiments under the same conditions end up in different final states characterised by different apparent masses. In the saturation regime, the relative fluctuations of apparent mass between configurations show a power-law decay as a function of the total number of grains $N^{-0.61}$.

I. INTRODUCTION

Granular media are systems composed of discrete macroscopic particles larger than $1 \mu\text{m}$, such as sand or rice. These media play an important role in areas such as agriculture, construction, geological phenomena (for example erosion), and even in the food industry. The most notable aspects of granular media are: first, that they are athermal systems, meaning that ordinary temperature does not play any role since thermal agitation is negligible; and secondly, the interactions between the grains in the system are dissipative in nature due to static friction and inelastic collisions [1]. Since thermal energy does not play a role in these systems, ordinary thermodynamic arguments do not necessarily apply, so in granular media, entropic considerations are secondary to dynamic effects, which become highly significant [1]. Moreover, since there are no thermal contributions, the system remains in metastable configurations for long periods of time unless some external perturbation is applied (e.g depending on how the container is filled, the packing fraction can vary between $\phi = 0.55$ and $\phi = 0.64$ in the case of hard spheres [2]). Therefore, granular packings would be expected to remain frozen in local states. However, it is well-known that the mechanical stability of granular systems slowly evolves in time, due to gravity and frictional forces.

In this work, experiments to address the slow dynamics of packed grains confined in vertical columns have been proposed. It can be observed that upon forming a column of grains of a sufficient height, the pressure at the base of the container does not increase. This occurs regardless of the additional amount of grains added, defining a maximum pressure value. This is the so-called “Janssen effect” [3]. This contrasts with the hydrostatic pressure in normal fluids. This unusual behaviour is the result of the action of contact and friction forces between grains and the container walls [3]. Contacts between grains can build up into force chains spanning across

the container diameter, thus sustaining the weight of the material above. Along these chains, the stresses are particularly intense [4]. These force chains can break and regenerate throughout time. Recently an anomalous behaviour has been reported where an overshoot in pressure (the measured mass exceeds the added mass into the cylinder) was observed in narrow containers before the saturation observed by Janssen [5]. This effect was named as the “Reverse Janssen effect” and was also observed to decrease as the tube diameter increased.

The aim of this work is to study the temporal evolution of granular systems formed by rigid spheres deposited inside a glass cylinder for large periods of time Δt .

II. MATERIALS AND METHODS

A. Experimental setup

The experimental setup consists of a cylindrical glass tube placed vertically sitting on two rigid bars so that the weight of the tube is not considered by a scale located

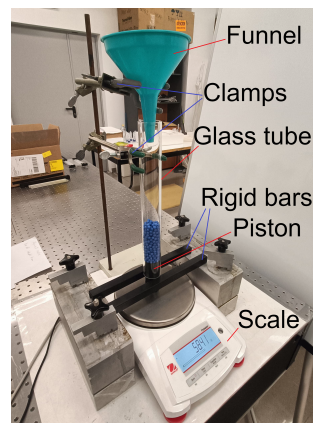


FIG. 1: Image of the experimental setup.

Tube	m_ℓ (g)	m_o (g)	m_s (g)
Small	5	17	30
Medium	6	60	85
Large	30	110	180

TABLE I: Imposed added mass, m , for the different tubes. m_ℓ is the mass corresponding to the liquid behaviour, m_o is the mass in the overshoot range and m_s the mass in the saturation regime.

directly below. Tubes of different diameters have been used: $D_S = 20.45 \pm 0.05$ mm, $D_M = 34.10 \pm 0.05$ mm, and $D_L = 49.15 \pm 0.05$ mm. Surrounding the container, a structure formed by clamps is placed to prevent the glass tube from falling. At the top of the structure, additional clamps hold a funnel through which the granular particles are deposited; this funnel also does not make contact with the glass tube. In order to measure “only” the granular material a piston is placed at the base connecting the grains with the scale Ohaus model Pioneer PX3202 with an uncertainty of ± 0.1 g. Figure 1 shows a picture of the experimental setup. A digital camera is placed on one side of the experiment to take pictures of the granular pile at a fixed time interval. Both, the camera and the scale are connected to a computer to record synchronously both images and weight.

The experiment consists of dropping a fixed mass of spheres made of plastic with a diameter $d_{\text{grain}} = 5.94 \pm 0.02$ mm and weight $m_{\text{grain}} = 112.6 \pm 0.1$ mg [5] and track the temporal evolution. These spheres exhibit a friction coefficient $\mu_{\text{grain}} = 0.3$ with the tube walls and with the other plastic spheres [6]. The duration of the experiments lasts between 6 and 10 hours. From now on, uppercase M will be used for measured mass using the scale placed at the bottom of the system, while lowercase m refers to actual added mass of grains inside the container. Three added masses, m , have been explored for each glass tube (see Table I). These values of m correspond to the different regimes observed when filling narrow containers adding δm at a fixed time step Δt : m_ℓ corresponds to liquid regime in which the apparent mass equals the added mass, m_o corresponds to the overshoot in pressure observed in the anomalous Janssen effect, and m_s corresponds to the saturation observed by Janssen (see Fig. 2).

B. Filling experiment

The filling protocol in “classical” Janssen experiments [3, 5] is different from the one used in the present work, where a fixed m is added and the system is allowed to evolve. In the original Janssen experiment the friction between the granular material and the container is at the Coulomb limit, while this is not the case in the present work. Even so, the classical filling protocol used by Janssen, served to identify the three interesting regimes discussed before: liquid-like m_ℓ , overshoot m_o ,

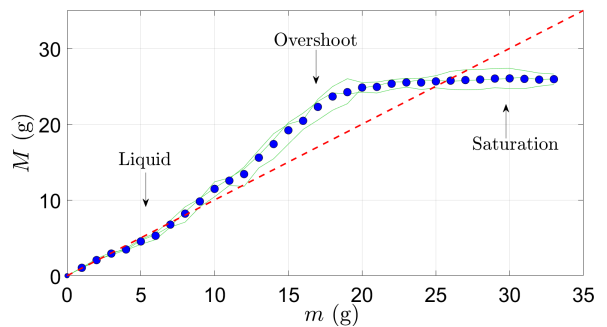


FIG. 2: Results of the Janssen experiment for the small tube with $\delta m = 1$ g. Blue dots correspond to an average over 3 different realisations shown as green lines. The red dotted line corresponds to a liquid-like behaviour. Three different regions can be distinguished: the first one corresponds to the liquid region where the granular behaviour is almost identical to the one of an hydrostatic system, the overshoot region where $M > m$ and the saturation region where M remains constant under the addition of more granular mass.

and saturation m_s ; which will be used for the temporal evolution experiment.

Figure 2 shows the results obtained by imposing $\delta m = 1$ g every $\Delta t = 2$ min using the small tube. This time interval allows the column of grains to reach equilibrium between different mass additions. δm is chosen to fill approximately a layer of grains inside the tube. For the different tubes δm changes between 1, 2.7 and 6 g for the small, the medium and the large tube respectively. M is recorded after Δt for each experiment and the data shown in Fig. 2 are the result of averaging over 3 different repetitions under the same experimental conditions. These results allows to identify the masses shown in Table I. The choice of these masses corresponds to different mechanical responses of the granular material in the container [5].

III. RESULTS

Figure 3 shows the temporal evolution of the small tube for added masses m_ℓ , m_o and m_s , in panels (a), (b) and (c) respectively. Equivalent representations have been obtained for the medium and the large tube. From the plots in Fig. 3 two regimes can be identified: (i) an initial mass relaxation, and (ii) a saturation of the measured mass at longer times. Figure 3 panel (c) highlights these two regimes. Some experiments show an increasing behaviour just after the first relaxation (as it can be seen in the blue curve of Figure 3 panel (b)). Even so, the common response of the experiments at sufficient long times is a saturation towards a stationary regime with fluctuations around a mean saturation mass M_{st} , which differs in each repetition of the experiment.

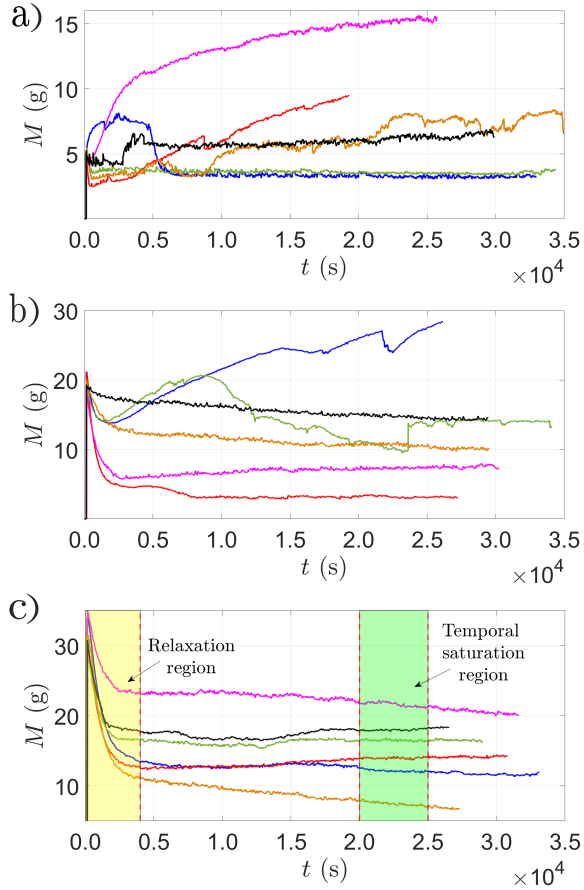


FIG. 3: Temporal evolution of the apparent mass M when adding an initial mass m_i inside the small tube. Panel (a) corresponds to the temporal evolution experiments using $m_\ell = 5$ g, (b) corresponds to the ones using $m_o = 17$ g, and (c) corresponds to the ones with $m_s = 30$ g. In this last panel can also be distinguished the different temporal regimes observed. Each curve represents each one of the six experiments done under the same conditions (same value of m_i and same glass tube).

A. Relaxation regime

A slow initial relaxation of the apparent mass M is observed in experiments conducted with added masses corresponding to m_o and m_s . This is not the case for experiments with m_ℓ where the relaxation occurs in a very short time.

The slow relaxation regime exhibited in experiments with m_o and m_s follows a decreasing exponential behaviour, similar to the discharge of a capacitor. Therefore, an exponential function of the form

$$M = Ae^{-t/\tau} + C \quad (1)$$

has been fitted to the experimental values of each experiment to extract the characteristic relaxation time τ . Experiments that exhibit subsequent increasing behaviour after the initial relaxation have not been analysed since

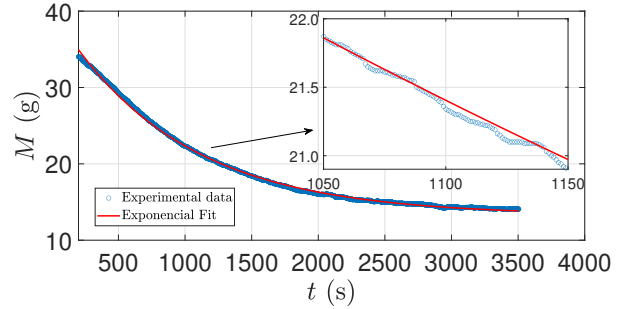


FIG. 4: Exponential fit to the experimental data of a single experiment for the small tube with $m_s = 30$ g (blue curve in Fig. 3 panel (c)). The inset shows a close up of the fit to the experimental data.

do not follow the general tendency. Figure 4 shows a fit to the data for a single experiment. The average values of τ for each tube are shown in Table II.

B. Fluctuations in the stationary regime

As pointed out before, at longer times the system reaches a saturation regime where the apparent mass fluctuates around a saturation mass M_{st} . These fluctuations have been characterised for each experiment over a time window of $\Delta t \approx 80$ minutes located at long times approximately around 6 hours (see Fig. 3). Figure 5 (a) shows a zoom to this saturation regime for a single experiment. In this figure it can be seen that the evolution of the apparent mass is characterised by a jerky signal (it has been tested that this fluctuating signal is not related with inherent fluctuations of the apparatus). The probability distribution is obtained for each experiment. An example is shown in Fig. 5 where panel (b) shows the probability of the fluctuations around the mean for the experiment with m_ℓ using the small tube. This distribution is obtained using the normalised variables

$$X_i = \frac{M_i - \bar{M}}{\sigma_M}, \quad (2)$$

where \bar{M} is the mean value of the fluctuations M_i and σ_M the standard deviation. This normalisation is done to compare the results with a normal distribution of 0 mean value and a standard deviation of one, $N(0,1)$. Similar results have been obtained for all the experiments done. However, experiments that showed a clear none

Tube	τ_o (s)	τ_s (s)
Small	$(8 \pm 3) \cdot 10^2$	$(9 \pm 1) \cdot 10^2$
Medium	$(9 \pm 2) \cdot 10^2$	$(9 \pm 3) \cdot 10^2$
Large	$(95 \pm 14) \cdot 10^1$	$(11 \pm 3) \cdot 10^2$

TABLE II: Average τ values for the added mass m_o (τ_o) and for m_s (τ_s) of the different tubes used.

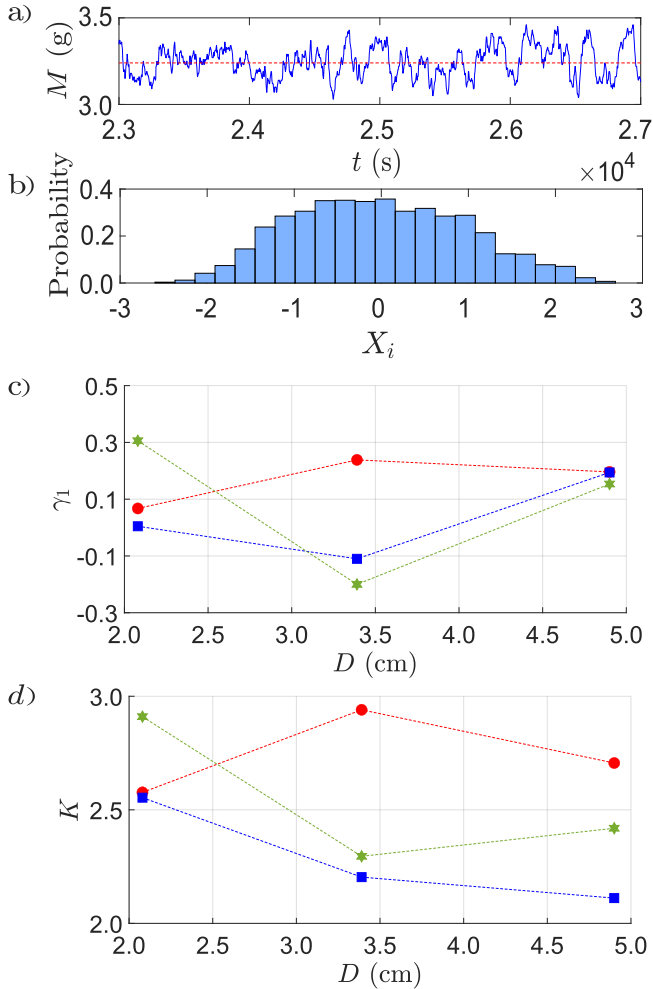


FIG. 5: (a) Fluctuations of the apparent mass (blue line) along the temporal saturation regime using the small tube and $m_\ell = 5$ g. The red dotted line corresponds to the mean value M in this time range. (b) Probability distribution calculated with the normalised fluctuations X_i . (c) and (d) show the evolution of the skewness (γ_1) and the kurtosis (K) as a function of the tube diameter for different values of m : m_ℓ red circles, m_o blue squares, and m_s green hexagons.

stationary trend, i.e. saturation was not reached and the system still evolves, have not been evaluated. For the extreme case of the largest tube this discrimination process has led to discarding most of the experiments conducted with m_s .

The normalisation in Eq. (2) imposes the values of the first and the second moment (mean and standard deviation) to 0 and 1 respectively. On the other hand, the skewness γ and the kurtosis K (third and fourth moments of the probability distribution) for comparison with those of a normal distribution $N(0,1)$, which should have values $\gamma_{1N} = 0$ and $K_N = 3$. These moments γ_1 and K are shown in Tab. III; and plotted as a function of the tube diameter in Fig. 5.

Moment m (g)	γ_1	K
5	0.10 ± 0.11	2.58 ± 0.18
17	0.0 ± 0.3	2.55 ± 0.14
30	0.3 ± 0.4	2.9 ± 0.2
6	0.2 ± 0.3	2.9 ± 0.5
60	-0.11 ± 0.19	2.2 ± 0.4
85	-0.2 ± 0.1	2.3 ± 0.2
30	0.2 ± 0.2	2.7 ± 0.6
110	0.19 ± 0.02	2.1 ± 0.5
180	0.15	2.4

TABLE III: Skewness γ_1 and kurtosis K calculated from the normalised fluctuations with form X_i , for each value of the added mass m . The errors bars correspond to the standard deviation of γ_1 and K between different repetitions of the experiment. Notice that the last value has no error bar since only one experiment displays a clear saturation state.

C. Fluctuations of M_{st} between realisations

As observed in Fig. 3, different realisations done under the same experimental conditions, end up in different temporal evolution with different saturation masses M_{st} , meaning that the system evolves into different final states. This is a common issue of athermal systems as it is with granular media. To account for the relevance of these variance between final states, the standard deviation between M_{st} of different realisations normalised by the actual added mass m_i , are plotted as a function of the number of grains in the container N in Fig. 6 (where $m_i \propto N$). The different relative standard deviations fall into a single curve that can be fitted as a decaying power-law, $\sigma/m \sim N^{-\alpha}$, as can be seen in Fig. 6. Figure 6 shows a fit to the data obtaining an exponent $\alpha = 0.61 \pm 0.07$.

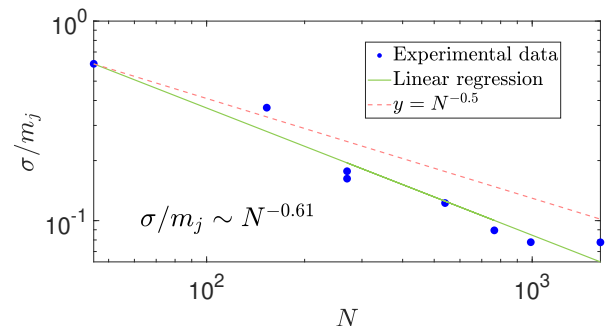


FIG. 6: Log-log plot of the experimental data and linear regression of σ/m as a function of the amount of grains N . The red dashed line corresponds to a guide to eye with of $y \sim N^{-0.5}$ for comparison.

IV. DISCUSSION AND CONCLUSIONS

This work presented a characterisation of the temporal evolution of confined granular matter. When adding grains into a cylindrical container the measured mass at the bottom showed an initial relaxation and mostly a saturation towards a stationary regime at longer times (some experiments show an increasing evolution of the measured mass). Measured mass is a proxy for the pressure at the bottom of the column.

In contrast with experiments with m_o and m_s , experiments performed at lower added masses, m_ℓ , show faster initial relaxation and a higher occurrence of an increase in the apparent mass M . The fast relaxation observed in m_ℓ can be originated by the fact that the medium does not develop force chain structures at these lower values of m . The relaxation observed in the different experiments performed with m_o and m_s , appears to be independent of the system volume. Table II shows that, as the values of τ present a large associated error, all of them can fall within an average characteristic relaxation time value of $(9 \pm 2) \cdot 10^2$ s (approximately 15 minutes).

At long enough times, the measured mass M saturates towards a stationary regime where M fluctuates around a saturation value, as seen in Fig. 5 panel (a). This fluctuating signal is characterised by skewness γ_1 with values close to 0, meaning that the probability distribution is symmetric, and a kurtosis K with values in the range of 2 to 3. The fact that K departs from 3 could be an indication of non-Gaussianity. Fluctuations that follow non-Gaussian distributions are typically indicative of the existence of internal correlations and/or intermittency, although in the latter cases $K > 3$ while the present set of experiments show $K < 3$. Non-Gaussian distributions have been reported in granular piles in previous experiments where the apparent mass fluctuates while the pile is regularly *tapped* [7].

In order to test if the fluctuations of apparent mass follow a non-Gaussian distribution, two tests, Kolmogorov-Smirnov and Lilliefors methods [8], have been applied to

X_i (Eq. (2)). These tests operate under the null hypothesis, which considers whether a sample comes from a given reference probability distribution, in our case whether the data comes from a Gaussian distribution. The rejection of this hypothesis implies that a relationship between our distribution and a normal distribution cannot be established [8]. When applying these two tests on the present data, both resulted in a rejection of the null hypothesis, implying, as has been well-commented above, that a relationship with a Gaussian distribution cannot be established.

Finally, it has been reported that the relative standard deviation of the apparent saturation mass between realisations with the same experimental conditions, σ/m , decay as the system approaches the thermodynamic limit as $N^{-\alpha}$ with $\alpha \approx 0.61$ (see Fig 6). So that the fluctuations of the observable M_{st} decay faster than expected, and this could be another indication that microscopic contributions to the macroscopic response are not independent.

To sum up the present set of results suggest that at saturation the apparent mass displays non-Gaussian fluctuations. However, the tests are inconclusive. In particular it would be interesting to perform additional experiments playing with the ratio D/d_{grain} and imposing different added masses m to explore different regimes to elucidate if this anomalous results can be supported.

Acknowledgments

Special thanks to my advisor Ramon Planet for the hours dedicated and for his invaluable guidance throughout this work. I would also like to thank my labmates for their assistance whenever I needed it, especially Adrià for his help at the beginning of the project. Finally, I am grateful to Marián Boguñá for helping me resolve some doubts that arose during the course of this work.

-
- [1] Jaeger H. M., Nagel S. R., and Behringer R. P. “Granular solids, liquids, and gases”. *Rev. Mod. Phys.* **68**: 1259 (1996).
 - [2] Onoda G. Y. and Liniger E. G. “Random loose packings of uniform spheres and the dilatancy onset”. *Phys. Rev. Lett.* **64**: 2727 (1990).
 - [3] Janssen, H. A. “Experiments on Corn Pressure in Silo Cells – Translation and Comment of Janssen’s Paper from 1895”. *Zeitschr. d. Vereines deutscher Ingenieure* **39**: 1045 (1895).
 - [4] Drescher, A. and De Josselin De Jong, G. “Stress transmission in granular matter”. *J. Mech. Phys. Solids* **20**: 337 (1972).
 - [5] Mahajan, S. et al. “Reverse Janssen Effect in Narrow Granular Columns”. *Phys. Rev. Lett.* **124**: 128002 (2020).
 - [6] Anderson, A.J. “Clusters, waves, and force chains in fire-ant collectives: emergent behavior in out-of-equilibrium particulate systems”. PhD. Thesis, Georgia Institute of Technology (2021).
 - [7] Nowak E. R., Knight J. B., Ben-Naim E., Jaeger H. M. and Nagel S. R. “Density fluctuations in vibrated granular materials” *Phys. Rev. E* **57**: 1971 (1998).
 - [8] Massey, F. J. “The Kolmogorov-Smirnov Test for Goodness of Fit.” *Journal of the American Statistical Association.* **46**: 68, (1951)